Journal Pre-proof

Application of statistical analyses for Lapis Lazuli stone provenance determination by XRL and XRF

Miriam Saleh , Letizia Bonizzoni Conceptualization Methodology , Jacopo Orsilli , Sabrina Samela , Marco Gargano , Salvatore Gallo , Anna Galli

Please cite this article as: Miriam Saleh , Letizia Bonizzoni Conceptualization Methodology , Jacopo Orsilli , Sabrina Samela , Marco Gargano , Salvatore Gallo , Anna Galli , Application of statistical analyses for Lapis Lazuli stone provenance determination by XRL and XRF, *Microchemical Journal* (2020), doi: https://doi.org/10.1016/j.microc.2020.104655

Highlights:

- XRF and XRL spectra were acquired on lapis lazuli stone samples

- Detected elements and bands are linked to geographical provenance of samples by comparison with literature data

- Statistical analyses considering both technique in the same elaboration have been then developed.

- Rough or polished sides of the same sample are always in the same group.

- Hierarchical Clustering on normalized area of the peaks/bands and whole spectra elaboration through SAM results in the same classification

Application of statistical analyses for Lapis Lazuli stone provenance determination by XRL and XRF

Miriam Saleh[a], Letizia Bonizzoni[a], Jacopo Orsilli[a], Sabrina Samela[a], Marco Gargano[a], Salvatore Gallo[a,b], Anna Galli[c,d]

[a] Dipartimento di Fisica "Aldo Pontremoli", Università degli Studi di Milano, via Celoria 16, 20133 Milano (Italy)

[b] Istituto Nazionale di Fisica Nucleare (INFN) sezione di Milano, via G. Celoria 16, 20133 Milano (Italy)

[c] Dipartimento di Scienza dei Materiali, Università degli Studi di Milano-Bicocca, via R. Cozzi 55, 20125 Milano (Italy)

[d] CNR-IBFM, via F.lli Cervi 93, 20090 Segrate (Italy)

Corresponding author: Letizia Bonizzoni, Dipartimento di Fisica, Università degli Studi di Milano, via Celoria 16, 20161 Milano (Italy).

letizia.bonizzoni@mi.infn.it

Abstract

Lapis Lazuli use stretches back more than 6,500 years; ancient civilizations of Mesopotamia, Egypt, China, Greece, and Rome treasured and prized it. Afghanistan has been the oldest source for this stone, while Chile, Canada, Russia and a few other countries have been reported as sources for raw material in more recent times; the rarity of historical mines surely represents a positive aspect for the provenance clue of artefacts. Lapis lazuli is a rock consisting mainly of lazurite, to which it owes the blue colour, calcite and pyrite. Other constituents may be present, related to the different mines. In the present work, we apply the principles of Radio-luminescence (RL) exploiting as radiation source the X-ray tube of a portable commercial X-Ray Fluorescence spectrometer; in this way, X-Ray Fluorescence spectra (XRF) can be simultaneously acquired to have a larger set of data. To highlight the instrumental experimental differences, we refer to the portable set up as X-Ray Luminescence (XRL), as suggested by recent literature. We thus looked for the possibility of applying a wieldy, low cost and non-destructive method that could fit also to precious objects, based on the join use of XRF and XRL. We performed analyses on raw Lapis Lazuli stones from five different provenances, both historical and modern, and on four sets of unknown origin carved polished stones, to test our methods on real artefacts. We focalised on a limited number of samples to concentrate on the statistical treatment of spectra obtained, so to get a synergic response of the two applied techniques. We were able to obtain a clear distinction for the different classified provenances and could speculate those of unknown samples.

Keywords

Radio-luminescence, X-Ray Fluorescence, X-Ray Luminescence, Lapis Lazuli provenance, MV analysis, SAM analysis

1 Introduction

Lapis lazuli is one of the first rock used by ancient civilizations: artefacts have been found in prehistoric tombs in Asia, Africa, and Europe. It is composed by different minerals; the principal one, which gives the blue colour, is lazurite. One of the mineral phases most commonly associated to it is

diopside, while other ancillary minerals can be calcite, pyrite, feldspars, wollastonite. Their presence may vary and may be related to lapis lazuli provenance [1]: in fact, different mineral phases in stones contains typical trace elements, that can be detected by means of elemental analyses, such as PIXE (Particle Induced X Emission) [2] or XRF (X-Ray Fluorescence) [3]. Exploiting the luminescence properties of minerals, also Ion Luminescence (IL) or Radio Luminescence (RL) can be used for provenance studies [4–6]. Recent papers have also proposed the application of XRL (X-Ray Luminescence) with the aim to go "towards a portable X-ray luminescence instrument for applications in the Cultural Heritage field" [7].

Lapis sources are rare, due to the peculiar geological conditions required for its forming [8]; notwithstanding, only few studies are focused on the determination of classification methods [9] or give an exhaustive characterization of old sources. This lack of systematic studies can be partially ascribed to the confusion about old sources as explained hereafter. Throughout the recorded use of lapis, the principal source has been in the Badakshan district of Afghanistan, which has been working for approximately six thousand years and has been mentioned frequently in historical documents. A Siberian deposit is located for sure at the southern end of Lake Baikal. The only other important locality is the Ovalle Cordillera (Andes Mountains), Coquimbo Province, Chile. Other localities of minor importance include sites in Myanmar, Colorado, and California.

In modern jewellery trade, various qualities of lapis lazuli are named after the region of origin, namely Chilean Lapis (the least valuable type; it contains numerous white calcite inclusions and is often tinged or spotted with green), Russian, or Siberian, Lapis (it contains pyrite, and is usually of good quality) and Persian Lapis, which is actually from Afghanistan (the finest, with little or no pyrite and no white calcite veining). Commercial names confirm the confusion about source locations: this also contributes to the difficulty in finding a correlation between mineral constituents and provenance. Most of the historical sources are located in quite inaccessible sites and it is not difficult to understand the dearth of eyewitness reports of activities at the mines, especially in old times. Indeed, many museums collections still show a lack of information about the exact provenance of stones [9]. Scientific literature also reports analyses on Lapis from Pakistan, Iran and Persia [10–12]. It worth noting that, from the geological point of view, Persia overlaps with nowadays Iran and a part of Iraq. Old manuscripts from XIII and XIV century, among which the diary of a Mongolian Empire emissary, report local mines, but they might be only a small quarry exhausted in the XIV century [13].

In this complex landscape, we looked for the possibility of applying a portable, low cost and non-destructive method that could fit also to precious objects, based on the join use of XRF and XRL. We developed then a statistical treatment of spectra obtained, so to get a synergic response of the two applied techniques. For this reason, we focalised on a limited number of samples, comparing results obtained by different data elaboration.

2 Materials and Methods

2.1 *Lapis lazuli samples*

Five different provenance lapis lazuli samples were selected to test the applicability of the proposed method, considering both polished and unpolished stones to verify whether the texture could interfere with classification. More than one point on each sample was considered, when possible, to take into account the intrinsic non-homogeneity of the rocks.

2.2.1 *Known origin samples*

Part of the known origin samples considered in the present work belongs to the Museum of mineralogical, gemmological and petrographic collections in the Department of Earth Sciences "Ardito Desio" of the University of Milan (UniMI). Samples from Afghanistan, Chile and Vesuvius were

acquired in 1937 from an older collection formed between the late XIX century and the early XX century: they come with their original labels attesting geological provenance. The Vesuvius sample original label reports also a question mark, denoting doubt about assigned provenance. The complete name "Vesuvius?" will be maintained throughout the present paper even if Mount Vesuvius is sometimes reported as a mining area for lapis lazuli, but only very small amounts in earthy state has been found [14–16]. Two more samples from the same Museum were acquired in the '60 for educational purposes; the given provenance is Canada and Persia. As stated in the introduction, Persian lapis lazuli are sometimes reported, but this source is not well documented. Moreover, the educational purpose mitigates in favour of an incorrect classification. Nonetheless, this sample is interesting as it is rough on the one side, and smooth on the other: four points have been considered on each side, so to verify the influence of surface texture.

Four more Afghan polished stones are from the Kremer set of raw materials for painting (40th anniversary, 2017) property of the Department of Material Science, University of Milano Bicocca (UniMIB). Again, particular attention has been given to the comparison with the raw Afghan older stone. Known samples features are summarized in table 1: in the following, they are used mainly to test our method.

2.2.2 Unknown origin samples

Some unknown stones have also been considered, to better test the classification capability of the proposed methods on real precious objects, as most of the techniques proposed in literature are not applicable in this peculiar case. The stones are mounted on pieces of jewellery from private collections and have not been disassembled. For these samples, only the purchase area is known; preliminary reflectance spectroscopy measurements have been conducted to confirm the geological nature of the stone. The four collections are set out in table 1.

Collection 1 is a complete parure, but single pieces show some differences in mounting. Namely, the ring has geometrical decorations instead of floral decorated filigree. The earrings and brooch mountings have different Cu/Au and Pb/Au ratio, as verified by XRF, even if the decoration of the metallic parts is very similar. Thus, it is possible that the set was originally not complete, and the stones themselves could be different: in fact, also appearance of stones shows some differences in the shades of blue and in the presence of gold colour speckles, very evident for instance in the ring stone. Regarding Collection 3, it has been produced and acquired in Ischia, an island near Naples, a region notorious for the carving of semi-precious stones and coral. Anyhow, a local origin (Vesuvius) for the stones can be excluded without any doubt, since no commercial exploitation of eventual local lapis lazuli quarry is attested. These sets of samples are intended to verify if our reference groups are able to classify unknown provenance stones.

2.2 Analytical techniques

Aiming to obtain a methodological approach exploiting a relatively low cost and portable instrumentation, a prototype was assembled, starting from a commercial portable XRF spectrometer and a luminescence detector. We applied the principles of Radio-luminescence (luminescence induced by X-Rays) exploiting as radiation source the X-ray tube of the portable commercial X-Ray Fluorescence spectrometer described in section 2.2.1; in this way, X-Ray Fluorescence spectra (XRF) can be simultaneously acquired to have a larger set of data. To highlight the instrumental experimental differences, we refer to the portable set up as X-Ray Luminescence (XRL) and to traditional laboratory one as RL (Radio-luminescence).

The described configuration allowed to perform XRF and XRL measurements on the exact same point of the samples. Due to the non-homogeneous geological structure of samples, several points on each stone were considered. We chose not to select a large number of samples, as we aimed to test if our statistical approach could help the description of analytical results in order to obtain a correlation with provenance information.

2.2.1 Portable X-Ray Fluorescence (p-XRF)
Assing model Lithos 3000 EDXRF portable spectrometer was chosen as its geometry eases the coupling with the luminescence spectrometer described in the next subsection. The p-XRF spectrometer is equipped with a low power X-ray tube with a Mo anode, that can be used both in monochromatic (100 μm Zr transmission filter, 4 mm radius on the sample) or polychromatic mode. Characteristic X-Rays are detected by a Peltier cooled Si-PIN detector and an interferometric system helps to maintain the sample–tube and sample–detector distances at 1.4 cm. The operating conditions were 25 kV and 0.3 mA, corresponding to the maximum power, with an acquisition time of 600 s for each measurement. Both quantitative analysis and areas deconvolution and calculation were performed using Assing Lab-Lithos software, after smoothing the spectra.

2.2.2 X-Ray Luminescence (XRL) and Radio Luminescence (RL)
Excitation of XRL was obtained exploiting the X-ray tube of XRF Lithos 3000 spectrometer, in the polychromatic mode (25 kV and 0.3 mA) collimated to obtain about 6 mm radius on the sample. The irradiated area and the positioning of the luminescence detector were verified by means of a ZnS foil. In a dark room, luminescence spectra were acquired by using a compact thermally cooled UV-Vis spectrometer (Prime X, B&WT TEK Inc. USA); the spectral range is 200-1000 nm and the resolution is approximately 1 nm. Integration time was set at 12500 ms with a 10 ms average integration time and 10 as multiplier factor. To collect the signals, Ocean optics 400 μm optical fibre bundle optimized for visible and infrared wavelength was used. Spectra were acquired without any white or black standard subtraction; peak areas were calculated with the dedicated software subtracting the baseline for each spectrum.
Planning *in situ* measurements, we used a low power X ray tube; for this reason, XRL spectra exhibit low intensity for the majority of samples (see. Par 3.2). To test the luminescence response of our samples, and thus verify the reliability of XRL results, RL has been performed on small fragments of two different provenances (Chile and Afghanistan). Analyses were carried out at room temperature (RT) using a home-made apparatus featuring, as detection system, a charge coupled device (CCD) (Jobin-Yvon Spectrum One 3000) coupled to a spectrograph operating in the 200-1100 nm range (Jobin-Yvon Triax 180) [17]. The data were corrected for the spectral response of the detection system. RL excitation was obtained by X-rays irradiation through a Be window, using a Philips 2274 X-ray tube with W target operated at 25 kV, 5mA with an acquisition time of 5s. Flakes were put in a modified sample holder, allowing small samples positioning (5 mm diameter, 1 mm height).

2.3 Statistical analyses
Statistical analyses were performed to try and get a provenance classification considering simultaneously both XRL and XRF results. This should make the classification method more effective than XRF and/or XRL technique considered alone, and easier to handle than *ex post* comparison.

2.3.1 Multivariate analysis
Multivariate analyses (namely Principal Component Analysis, PCA, and Hierarchical Clustering, (HC) were performed considering areas for each XRF peak and XRL band. Areas were calculated as

explained in section 2.2.1; moreover, XRF signals were normalized to measuring time and Rayleigh scattering peak to take into account differences in the geometry of the samples. For PCA, correlation matrix was used; correspondingly, standardization of data was applied for HC analysis (ward linkage, Euclidean distance). This procedure was chosen so to weigh signals corresponding to trace elements/minerals as much as prevailing ones [18]. In the following of the present paper, only significant output graphics will be reported.

2.3.2 Spectral Angle Mapping

Spectral data have been analysed through SAM (Spectral Angle Mapper) automated method classification. In this technique, usually applied to study geospatial images [19], each spectrum is considered as a multidimensional point in a $n \times n$ space, where n is the number of spectrum channels. This allows to directly compare spectra treating them as vectors and calculating the spectral angle between them. If we consider the vectors from the origin to the spectral points, we can define the distance between the two points as the angle between the two vectors. In this way, the distance between two spectra is computed as:

$$\alpha = \arccos\left(\frac{\sum_{i=1}^{n} r_{i,1} r_{i,2}}{\left(\sum_{i=1}^{n} r_{i,1}^2 \sum_{i=1}^{n} r_{i,2}^2\right)^{\frac{1}{2}}}\right)$$

where r_1 e r_2 are the coordinates (the value of each channel) of the spectra considered. Similar spectra have a smaller angle, while different spectra will have a higher angle value. To take into account both technique outputs, the XRF and XRL spectra of each sample have then been joined to create a unique spectrum with n+m channels (n channels from XRF and m channels from XRL).
To perform the analysis, XRF spectra have been previously normalized to the Rayleigh peak area as for the multivariate analysis so to take into account the different sample geometry, while XRL spectra have been divided over the background in a region without signals.
This kind of data handling has already been applied to whole spectra in the analysis of multispectral data in the UV-Vis-NIR range [20]. In that case, some problems arose due to the nature of the spectra which may have both absorption and reflection bands. In the present research, instead, the peculiar shape of XRF and XRL spectra, composed only of emission peaks in precise ranges, overcomes this limit.

3 Results and discussion
Spectra obtained both by XRF and XRL have been at first separately considered and compared with literature data. Statistical analyses considering both technique in the same elaboration have been then developed.

3.1 XRF results
XRF analyses have been performed over areas of about 4 mm radius on the sample; this implies an average answer on the different minerals composing rocks. Moreover, for each sample, more than one point was considered, so to have a representative description of the sample itself. Most part of literature data [3,9] refers to microanalyses, which allowed selecting one mineral phase. Nonetheless, some useful information can be obtained by comparison, on the bases of data reported in table 2.
Overall element detected on reference stones by XRF were Cl, Ag, K, Ca, Ti, Mn, Fe, Zn, Ga, Pb, Rb, Sr, Au, Br. Cr and Cu were also present, but resulted always under minimum detection limits (MDL:

0.02% for Cu and 0.03% for Cr) for all samples. Table 2 shows the averaged concentration of quantifiable elements for each assigned known provenance. Due to the heterogeneity of samples, data scattering can be as high as 30% in worst cases.

Cl traces were detected only in Canadian sample, together with Br; Ag characterized the five Afghan samples while Au was detected only in the polished Afghan samples and for this reason its average amount is below MDL (0.02%) and it is not reported in table 2. The raw Afghan stone was mined before the end of XIX century, while the polished stones are from the present century; this can be an explanation for those minute variations in trace elements. All the Afghan samples, coherently with general knowledge about commercial lapis from Afghanistan (see Introduction), show very low amount of Fe and relatively low concentration of Ca. On the opposite, the supposed Vesuvius sample shows a considerable content of Fe and Sr, about one order of magnitude higher than all other provenances. Other authors [1,4,9] demonstrate that high contents of Fe and Sr in diopside are typical of Siberian lapis lazuli and, among commercial qualities, Siberian Lapis (see Introduction) is characterized by a high amount of pyrite, and consequently of Fe. This can be a hint for the real provenance of this sample, that in the following will be nonetheless called "Vesuvius?". Chile and Persia samples all present relatively high concentration of Ca and Fe, with a close average concentration. Spectra obtained for Chilean and Afghan stones are reported in fig. 1a.

3.2 XRL results

Due to the low power tube used for luminescence excitation, XRL spectra show an average low intensity. Being the radio luminescence correlated to the presence and structure of defects in the analysed material, in principle, the emission spectra carry information about the recombination sites involved in the luminescence processes. Interpretation of spectra from natural samples is very complicated compared with those from relatively pure crystals. First, the luminescence of a given ion strongly depends on its position in the crystal. Hence, an ion can produce a great variety of luminescence spectra. Secondly, natural samples contain a great variety of different centres that give rise to complex spectra that are difficult to interpret. Therefore, at this stage of our research we focus our attention on the presence of main bands, and not on the individuation of the single luminescence centre. Spectra obtained for Chile and Afghanistan samples are reported in fig. 1b.

Particular attention was also given to the sample classified as Persian: four points were considered on the raw face and four on the polished one. No significant differences were detected, as it is evident in the statistical analysis output (see. 3.3).

Bands used for samples classification are reported in table 3 for known provenance samples, together with average band areas for different provenances calculated as stated in section 2.2, showing a qualitative differentiation.

Bands from 565 nm to 715 nm have been indicated in literature [7] as useful for XRL characterization. Our experimental device shows a good sensitivity also at lower wavelength until the UV region, allowing a more extended range of detection and the possibility of exploit also UV bands. Moreover, the good resolution on our detector gives narrow and well-defined peaks even when low in intensity. All of our Afghan samples can be clearly discriminate for their change of slope at about 500 nm, resulting in a very broad band from this wavelength on [7]; this must be considered when arguing about bands with wavelength higher than 500 nm for Afghan lapis.

3.2.1 RL results

We performed Radio Luminescence on two flakes taken from the Chilean lapis and one from the polished Afghan stone, thus considering the two main historical sure sources among our samples. This was performed mainly to test the luminescence response of considered stones, and thus verify the

reliability of XRL results. Spectra obtained are reported in fig. 1c. Chile spectrum shows a main composite emission band centred at 560 nm that can be referred to wollastonite, peculiar of Chile sample [4] and a blue band (λ_{MAX} = 450 nm) probably ascribable to the presence of feldspars, coherently with the high Ca concentration detected by XRF.

For the Afghan sample, the RL spectrum is more complex; in the UV-blue region there are two emission centred at 400 nm, typical for the lapis coming from the Asian region [21], and at 480 nm, respectively. At 580 nm there is a band, probably ascribable to diopside, an accessory mineral of lazurite; this band is also present in the XRL spectra of Afghan samples. Moreover, in RL spectra, there are two broad bands centred respectively at 730 and 950 nm. These bands do not find any correspondence in XRL spectra, as for wavelength higher than 714 nm, the rise of the background is prevalent.

3.3 Statistical data handling

Multivariate Analyses were applied first to the set of known origin samples and later to the total number of samples investigated. We applied both PCA and HC considering peak areas, calculated as state in section 3.2 as variables. We made a preliminary statistical elaboration considering all the elements and bands detected; on the bases of loading plots and clusters variables (grouping the variables for their similarity), we chose the most statistically meaningful energies and/or wavelengths, to eliminate noise from our data. Ag, Au and Pb were excluded from XRF detected elements, also because the metal mounting of jewels could influence their presence. From XRL spectra, bands considered were 283, 545, 610, 670 and 714 nm. The last wavelength allowed taking into account the characteristic rising of Afghan samples we accounted for in section 3.2. To exploit the synergy between XRF and XRL, both XRL bands and XRF peak areas were considered as variables in the same data elaboration. To make variables homogeneous and to give the same weight to less intense peaks/bands, we applied standardization of data. PCA (correlation matrix) results reflected HC dendrogram (Ward linkage, Euclidean distance), but variance explained for the first three principal components was only about 66%; for this reason, only HC output are reported in the following. We also tested spectral angle mapper (SAM) on the entire spectra: this allowed us to take into account all the bands/elements detected and the peculiar background of Afghan Lapis. SAM elaboration could be applied only to known provenance samples for the influence of metal alloys on XRF spectra for artefacts.

3.3.1 Known provenance samples

Fig. 2 shows the dendrogram obtained for the selected signals from both XRF and XRL (see above) of known samples provenance. Four groups are evident: the one of Canadian samples (codes 1, 2, 3), the Afghan samples (12, 19, 20, 21, 22), Persia and Chile (4-11, 13-16), "Vesuvius?" (17, 18). This classification proves the possibility of considering in a unique statistical elaboration both XRF and XRL data, and confirms the wrong origin of Persian samples (4-11), suggesting instead a Chilean provenance. The two subgroups in Chile/Persia group do not reflect the supposed provenance nor the texture. Indeed, it is interesting to note that all measurements on rough and polished sides of the Persian sample fall in this one group; in the same way, various Afghan samples with different textures and mining periods pertains to a unique group.

Supporting these results, output from SAM elaboration of spectra is reported in fig. 3. Spectra have been processed as explained in section 2.3.2. Moreover, as XRL spectra have a low signal to noise ratio, they have been further weighted so that the higher XRL bands have a similar intensity to XRF peaks, and XRL spectra noise is of the same order of magnitude as XRF spectra noise. We then calculated the SAM of every combination of two spectra, obtaining the distance matrix. The dendrogram has been extracted using Euclidean distance and complete linkage. Both distance matrix

(higher similarity, darker color) and dendrogram are reported in fig. 3. The obtained five groups reflect those from chemometric data elaboration (see fig 2). The first (samples 17, 18 in purple) contains the "Vesuvius?" sample, the second and the third groups (in dark red) contains the Chilean and the Persian samples, mixed up; the fourth group (samples 1, 2, 3 in blue) the Canadian samples, and the last (samples 12, 19, 20, 21, 22 in green) the Afghan lapis lazuli.

3.3.2 Classification of unknown provenance samples

The next step of our elaboration was the application of our verified approach to the unknown samples, considering the same variables as fig 3; Ward linkage and Euclidean distance were applied (fig.4). SAM analysis was not relevant for the presence of Au, Ag and Cu signals from metallic mounting in XRF spectra of jewels.

The four groups of figure 3 are maintained, also for Chile/Persia Lapis. Unknown samples spread over the three groups referring to the three modern commercial types of stones - that is Afghanistan, Chile and Siberia (corresponding to our "Vesuvius?" sample) - as expected being non archaeological objects. More in detail, the most recent artifacts (collection 2 and 3) pertain to the Chilean group, the less expensive among modern sources. Only two samples are described by statistical analysis as from the most valuable provenance, Afghanistan: the small egg (collection 4) and the brooch of collection 1. The remaining part of collection 1 divides among Chile and Siberian groups. In Chile group are sample 29, the ring, with a different mounting decoration, and the stones from the bracelet, except one, that is sample 27. The two earrings (with a different metal alloy from the brooch) and one stone from the bracelet falls in the "Vesuvius?" group: thus, the most possible provenance for them is Siberia. Obviously, the presence of a fifth provenance for some of the unknown samples cannot be *a priori* excluded.

4. Conclusions

The new methodological approach presented in this work proved to be suitable for the classification of both raw and polished lapis lazuli stones. XRF and XRL spectra information were accounted together in the same statistical elaboration, considering both normalized area of the peaks/bands through traditional HC analysis and whole spectra through SAM. For SAM elaboration, the low signal to noise ratio forced us to weighted spectra so to emphasise only higher signals, as the smaller ones confuse with the background. This suggests the necessity to improve this ratio for future experiments. Moreover, based on the obtained spectra, we were able to recognize fake provenance assignments and to suggest the correct one for some raw samples. A higher number of reference samples, covering all the possible historical and modern provenances, will be considered in the next future for the creation of a useful database; for this aim, unsure provenance reference samples should be avoided. About classification results, it is interesting to note that measurements on rough or polished sides of the Persian sample are always in the same group; likewise, Afghan samples with different textures (one rough, four polished), and mining periods (more than one century) all pertains to one group.

Declaration of interests

☒ The authors declare that they have no known competing financial interests or personal relationships that could have appeared to influence the work reported in this paper.

Sample CRediT author statement

Miriam Saleh	Investigation, Validation, Formal analysis
Letizia Bonizzoni	Conceptualization, Methodology, Writing - Review & Editing, Supervision
Jacopo Orsilli	Software, Visualization
Sabrina Samela	Investigation
Marco Gargano	Investigation
Salvatore Gallo	Resources
Anna Galli	Resources, Investigation, Validation

References

[1] A. Re, A.L. Giudice, D. Angelici, S. Calusi, L. Giuntini, M. Massi, G. Pratesi, Lapis lazuli provenance study by means of micro-PIXE, Nuclear Instruments and Methods in Physics Research Section B: Beam Interactions with Materials and Atoms. 269 (2011) 2373–2377. doi:10.1016/j.nimb.2011.02.070.

[2] A. Re, D. Angelici, A.L. Giudice, E. Maupas, L. Giuntini, S. Calusi, N. Gelli, M. Massi, A. Borghi, L.M. Gallo, G. Pratesi, P.A. Mandò, New markers to identify the provenance of lapis lazuli: trace elements in pyrite by means of micro-PIXE, Appl. Phys. A. 111 (2013) 69–74. doi:10.1007/s00339-013-7597-3.

[3] D. Angelici, A. Borghi, F. Chiarelli, R. Cossio, G. Gariani, A. Lo Giudice, A. Re, G. Pratesi, G. Vaggelli, μ-XRF Analysis of Trace Elements in Lapis Lazuli-Forming Minerals for a Provenance Study, Microsc. Microanal. 21 (2015) 526–533. doi:10.1017/S143192761500015X.

[4] A.L. Giudice, A. Re, S. Calusi, L. Giuntini, M. Massi, P. Olivero, G. Pratesi, M. Albonico, E. Conz, Multitechnique characterization of lapis lazuli for provenance study, Anal Bioanal Chem. 395 (2009) 2211–2217. doi:10.1007/s00216-009-3039-7.

[5] M. Dowsett, M. Hand, P.-J. Sabbe, P. Thompson, A. Adriaens, XEOM 1 - A novel microscopy system for the chemical imaging of heritage metal surfaces, Herit Sci. 3 (2015) 14. doi:10.1186/s40494-015-0042-5.

[6] J. Götze, Potential of cathodoluminescence (CL) microscopy and spectroscopy for the analysis of minerals and materials, Anal Bioanal Chem. 374 (2002) 703–708. doi:10.1007/s00216-002-1461-1.

[7] A. Re, M. Zangirolami, D. Angelici, A. Borghi, E. Costa, R. Giustetto, L.M. Gallo, L. Castelli, A. Mazzinghi, C. Ruberto, F. Taccetti, A.L. Giudice, Towards a portable X-ray luminescence

instrument for applications in the Cultural Heritage field., Eur. Phys. J. Plus. 133 (2018) 362. doi:10.1140/epjp/i2018-12222-8.

[8] L. von Rosen, Lapis lazuli in geological contexts and in ancient written sources, P. Åström, 1988.

[9] A.L. Giudice, D. Angelici, A. Re, G. Gariani, A. Borghi, S. Calusi, L. Giuntini, M. Massi, L. Castelli, F. Taccetti, T. Calligaro, C. Pacheco, Q. Lemasson, L. Pichon, B. Moignard, G. Pratesi, M.C. Guidotti, Protocol for lapis lazuli provenance determination: evidence for an Afghan origin of the stones used for ancient carved artefacts kept at the Egyptian Museum of Florence (Italy), Archaeol Anthropol Sci. 9 (2017) 637–651. doi:10.1007/s12520-016-0430-0.

[10] A. Borelli, C. Cipriani, C. Innocenti, R. Trosti, Caratterizzazione del lapislazzuli, La Gemmologia, XI. 24 (1986) 27.

[11] C. Cipriani, C. Innocenti, R. Trosti-Ferroni, Le collezioni del museo di mineralogia di Firenze: VI) i lapislazzuli, Museologia Scientifica, V. 17 (1988) 30.

[12] P. Ballirano, A. Maras, Mineralogical characterization of the blue pigment of Michelangelo's fresco "The Last Judgment," American Mineralogist. 91 (2006) 997–1005. doi:10.2138/am.2006.2117.

[13] Ḥamd Allāh Mustawfī Qazvīnī, G. Le Strange, The geographical part of the Nuzhat-al-qulub, London : E.J. Brill, Luzac & Co., Leyden, 1915.

[14] R.J.H. Clark, M.L. Curri, C. Laganara, Raman microscopy: The identification of lapis lazuli on medieval pottery fragments from the south of Italy, Spectrochimica Acta Part A: Molecular and Biomolecular Spectroscopy. 53 (1997) 597–603. doi:10.1016/S1386-1425(96)01768-4.

[15] E.S. Dana, W.E. Ford, A Textbook of Mineralogy, 4th edition, Wiley, New York etc., 1991.

[16] C. da Cunha, Le Lapis Lazuli : Son histoire, ses gisements, ses imitations, Editions du Rocher, Paris, 1989.

[17] A. Galli, M. Martini, E. Sibilia, G. Padeletti, P. Fermo, Luminescence properties of lustre decorated majolica, Appl. Phys. A. 79 (2004) 293–297. doi:10.1007/s00339-004-2517-1.

[18] L. Bonizzoni, A. Galli, M. Gondola, M. Martini, Comparison between XRF, TXRF, and PXRF analyses for provenance classification of archaeological bricks, X-Ray Spectrometry. 42 (2013) 262–267. doi:10.1002/xrs.2465.

[19] J. Weyermann, D. Schläpfer, A. Hueni, M. Kneubühler, M. Schaepman, Spectral Angle Mapper (SAM) for anisotropy class indexing in imaging spectrometry data, in: Imaging Spectrometry XIV, International Society for Optics and Photonics, 2009: p. 74570B. doi:10.1117/12.825991.

[20] P.R. Meneses, Spectral Correlation Mapper (SCM) : An Improvement on the Spectral Angle Mapper (SAM), in: 2000.

[21] A. Lo Giudice, A. Re, D. Angelici, S. Calusi, N. Gelli, L. Giuntini, M. Massi, G. Pratesi, In-air broad beam ionoluminescence microscopy as a tool for rocks and stone artworks characterisation, Anal Bioanal Chem. 404 (2012) 277–281. doi:10.1007/s00216-012-6110-8.
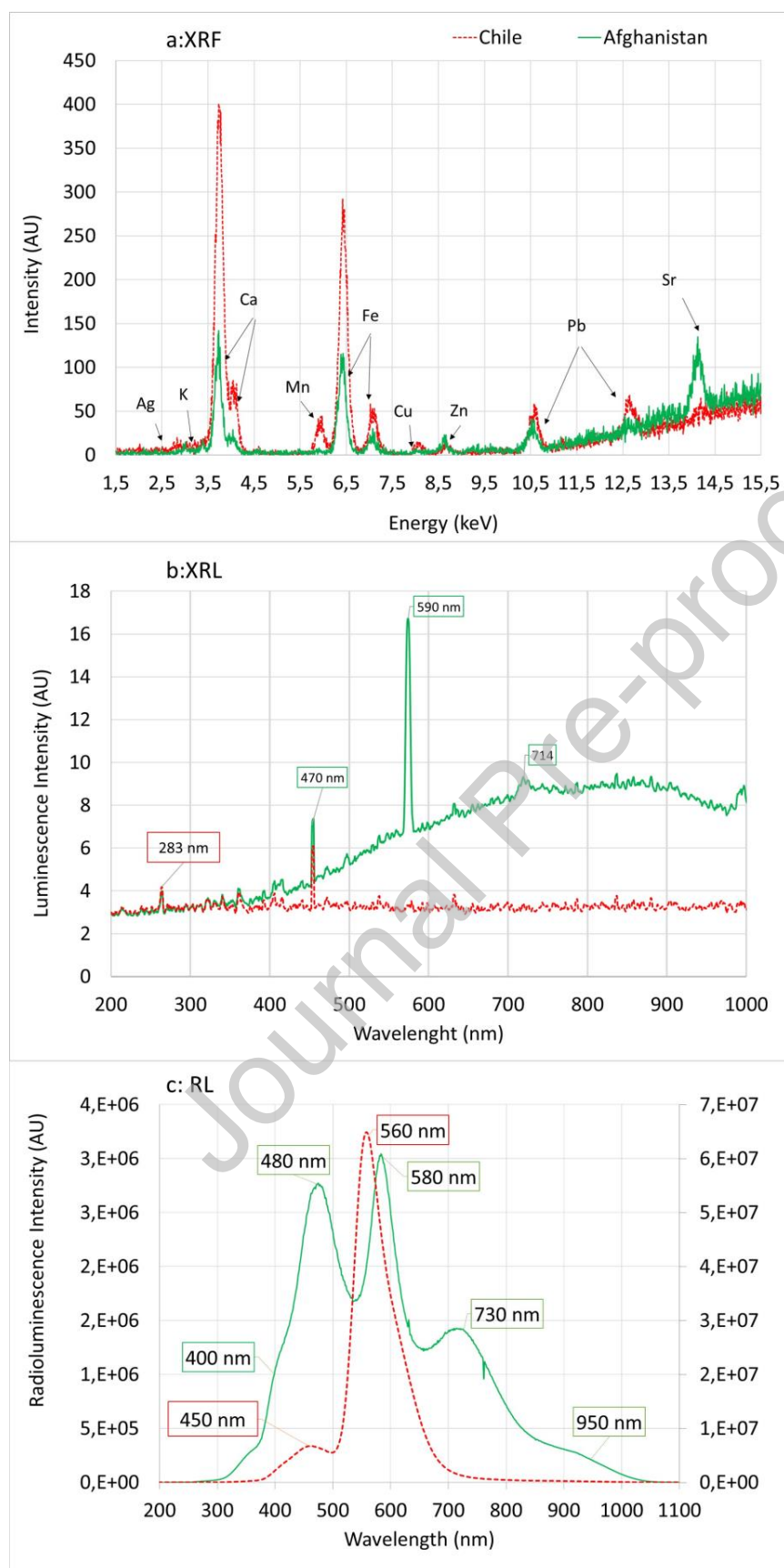
Figure captions

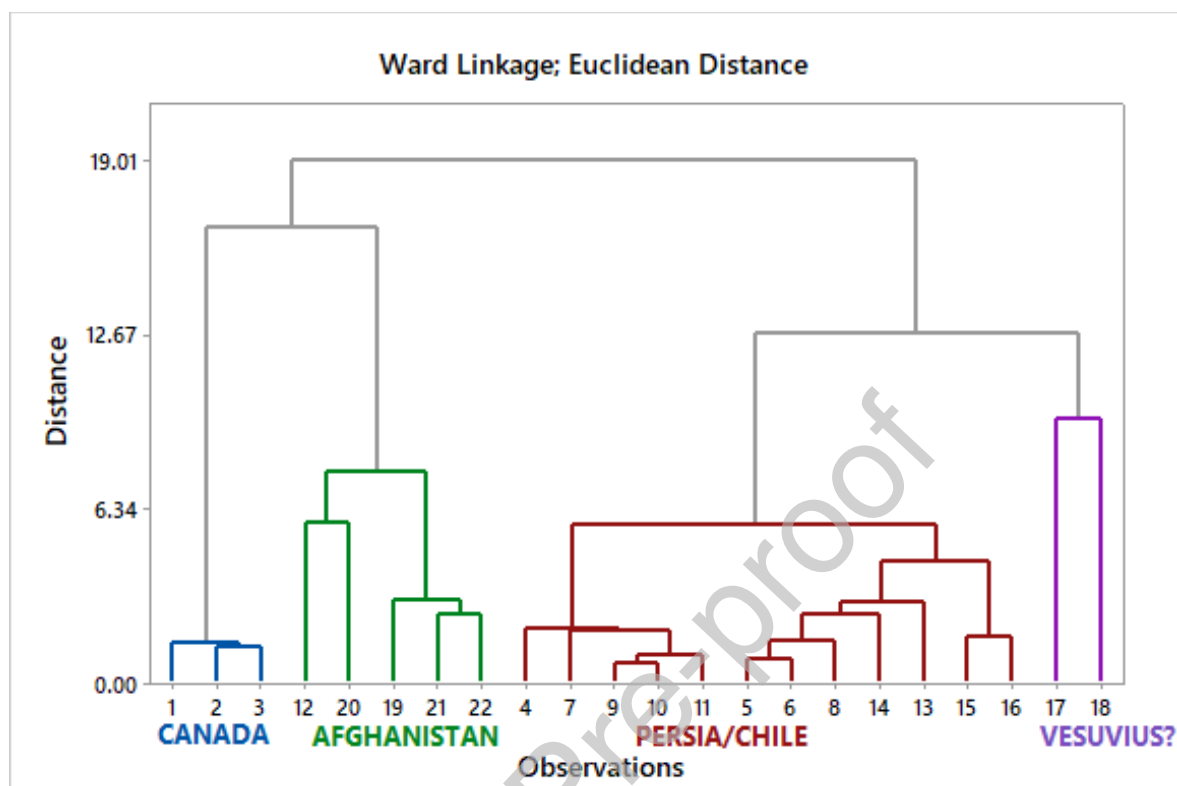**Fig.1.** XRF (1a), XRL (1b) and RL (1c) spectra for Chile and Afghanistan samples.

Fig.2. Dendrogram of known provenance samples obtained from standardized areas of signals at 283, 545, 610, 670, 714 nm (XRL) and peak areas of Cl, K, Ca, Ti, Mn, Fe, Zn, Ga, Rb, Sr, Br (XRF). Ward Linkage and Euclidean distance have been applied.

Fig. 3. Distance matrix and dendrogram (Euclidean distance, complete linkage) of known provenance samples obtained from the elaboration of XRF and XRL whole spectra, standardized and weighted to make them comparable. Sample Labels are marked near the low and right axes.

Fig. 4. Dendrogram of known and unknown provenance samples obtained from standardize areas of signals at 283, 545, 610, 670, 714 nm (XRL) and peak areas of Cl, K, Ca, Ti, Mn, Fe, Zn, Ga, Rb, Sr, Br (XRF). Ward Linkage and Euclidean distance have been applied.
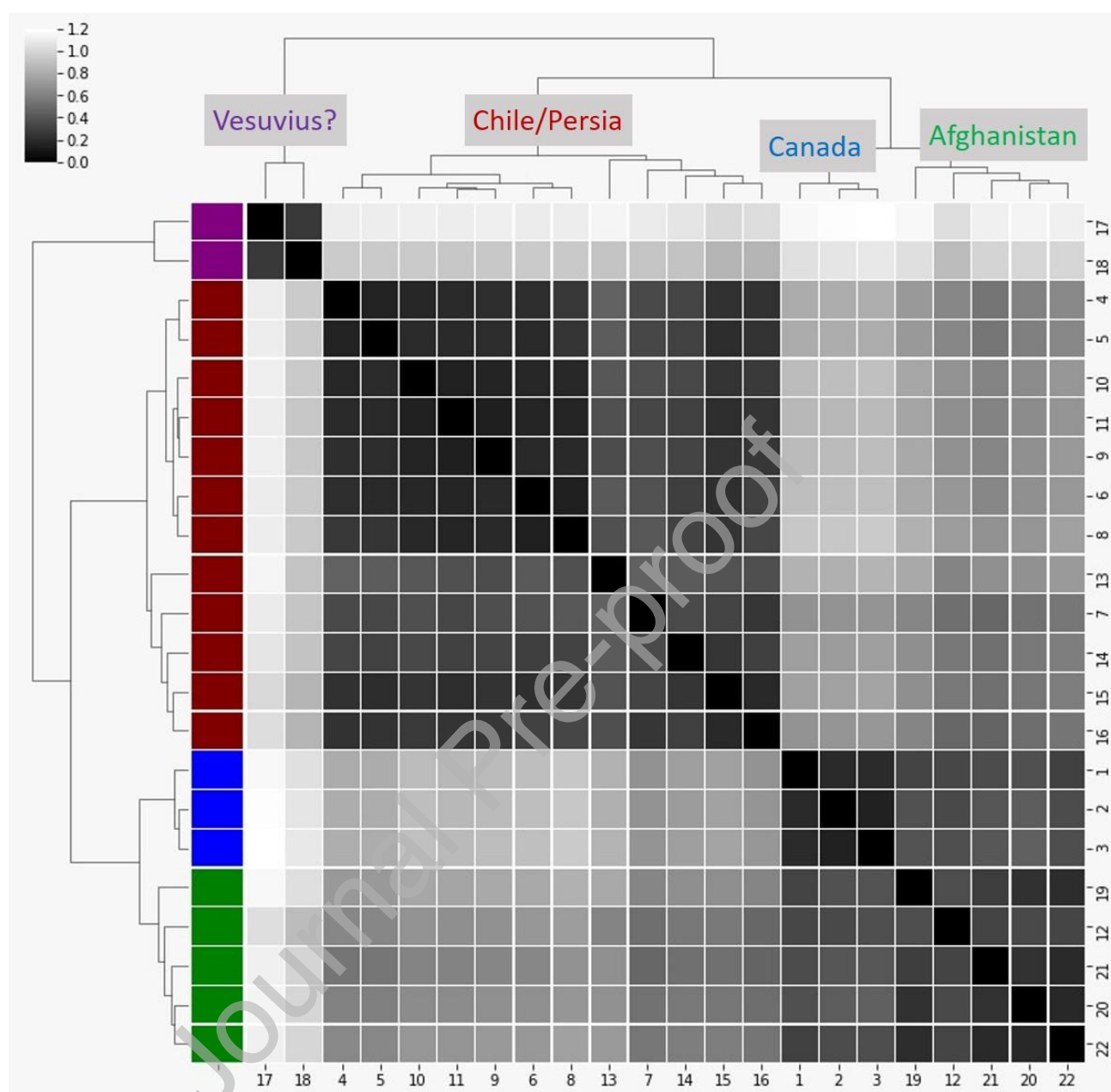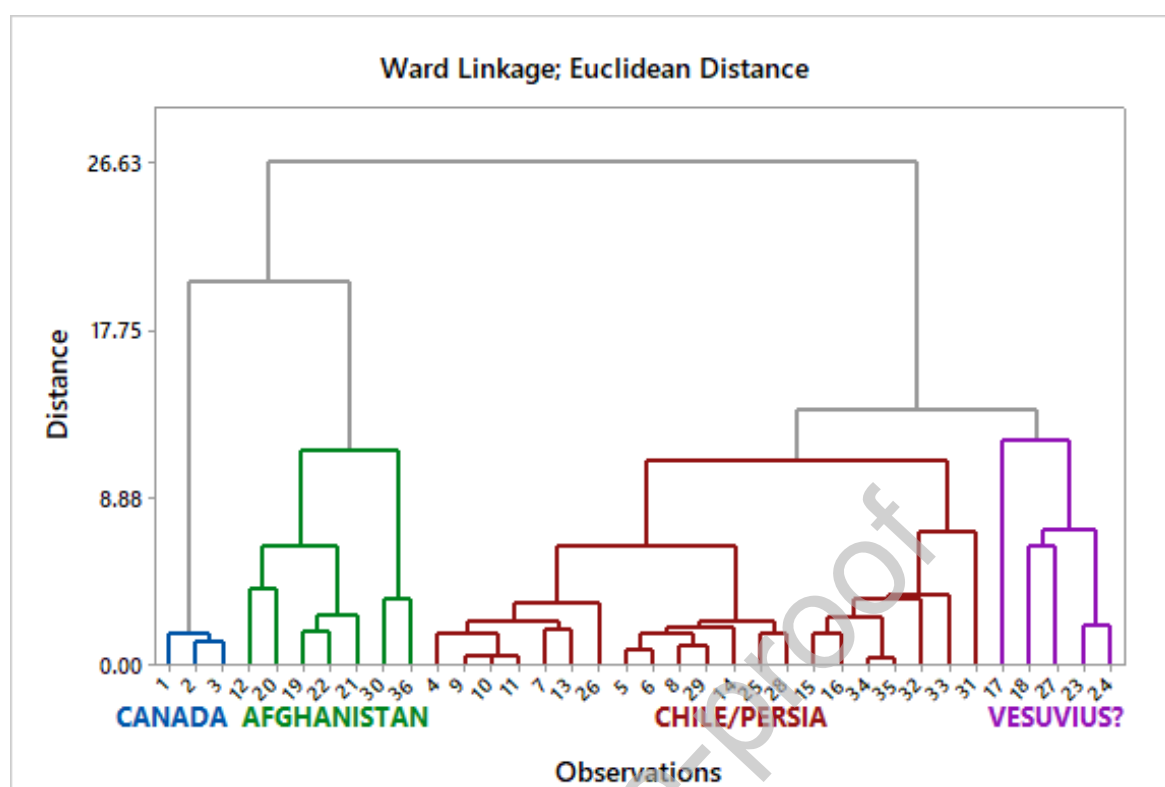
15

Table 1: Known and unknown provenance samples list; in the first column, the numbers refer to the measure numbers in statistical analysis output. For private collections, the region of purchasing is reported.

MV Code	Provenance	Property	Picture	Max Dimensions (mm)	Features
1/3	Canada	Department of Earth Sciences, UniMI		47.8 x 26.2 x 24.2	Rough. Bright and opaque blue area.
4/11	Persia	Department of Earth Sciences, UniMI		25.9 x 13.0 x 7.9	One side rough, one side polished. Blue area with white inclusion.
12	Afghanistan	Department of Earth Sciences, UniMI		44.0 x 30.7 x 19.1	Rough. Small intense blue areas.
13/16	Chile	Department of Earth Sciences, UniMI		85.3 x 46.9 x 37.4	Rough. Blue parts quite homogeneous with small light blue inclusions.
17/18	Vesuvius(?)	Department of Earth Sciences, UniMI		44.2 x 40.6 x 25.1	Rough. Light blue area with grey inclusions.
19	Afghanistan	Department of Material Sciences, UniMIB		17.2 x 9.2 x 14.8	Polished, rounded. White inclusions.
20	Afghanistan	Department of Material Sciences, UniMIB		10.6 x 5.1 x 7.9	Polished, rounded.
21	Afghanistan	Department of Material Sciences, UniMIB		25.6 x 4.3 x 11.5	Polished, rounded and flat.
22	Afghanistan	Department of Material Sciences, UniMIB		22.1 x 8.7 x 11.4	Polished, rounded and flat.
23	Unknown	Collection 1 Northern Italy		15.1 x 6.4 x 11.4	Earring, cabochon
24	Unknown	Collection 1 Northern Italy		15.1 x 6.4 x 11.4	Earring, cabochon
25/28	Unknown	Collection 1 Northern Italy		17.6 x 10.3 x 13.8	Bracelet, 4 cabochon
29	Unknown	Collection 1 Northern Italy		17.6 x 10.3 x13.8	Ring, cabochon
30	Unknown	Collection 1 Northern Italy		16.6 x 10.4 x 13.8	Brooch, cabochon
31	Unknown	Collection 2 Morocco		20.1 x 15.6 x 7.0	Ring, cabochon
32	Unknown	Collection 3 Ischia, Italy		18.9 x 18.2 x 6.9	Earring, cabochon
33	Unknown	Collection 3 Ischia, Italy		18.9 x 18.2 x 6.9	Earring, cabochon
34/35	Unknown	Collection 3 Ischia, Italy		18.9 x 18.2 x 6.9	Necklace, 2 cabochon considered
36	Unknown	Collection 4 Unknown		44.7 x 34.2 x 34.2	Polished, egg-shaped

Table 2: XRF results: averaged concentration of quantifiable elements for each assigned known provenance. Last row reports Minimum Detection Limit for each element considered.

	Cl (%)	Ag (%)	K (%)	Ca (%)	Ti (%)	Mn (%)	Fe (%)	Zn (%)	Ga (%)	Pb (%)	Rb (%)	Sr (%)	Br (%)
Canada	6.77	<MDL	0.57	0.64	0.05	0.04	0.13	<MDL	0.01	0.05	<MDL	<MDL	0.05
Persia	<MDL	0.79	0.98	20.37	0.56	0.04	0.36	0.01	<MDL	0.04	<MDL	0.02	<MDL
Afghanistan	<MDL	1.50	2.95	8.07	0.20	<MDL	0.08	<MDL	<MDL	<MDL	0.01	0.02	<MDL
Chile	<MDL	<MDL	0.57	18.03	0.32	0.11	0.46	<MDL	<MDL	0.02	<MDL	0.02	<MDL
Vesuvius?	<MDL	<MDL	2.74	24.19	0.39	0.19	1.56	0.02	<MDL	<MDL	0.01	0.37	<MDL
MDL	0.36	0.33	0.13	0.11	0.03	0.03	0.03	0.01	0.02	0.02	0.01	0.01	0.01

Table 3: XRL results: averaged areas of luminescence bands for each assigned known provenance; wavelength reported correspond to the maximum of intensity.

	283 nm	295 nm	311 nm	350 nm	380 nm	402 nm	422 nm	434 nm	470 nm	484 nm
Canada	0.00	9.70	6.68	5.03	4.45	4.11	7.19	0.00	5.72	5.10
Persia	5.90	5.96	6.66	5.05	3.81	3.68	7.23	1.66	7.14	7.77
Afghanistan	6.39	5.60	6.61	0.00	1.02	0.38	7.43	1.35	5.03	5.04
Chile	6.11	4.80	5.82	5.01	3.89	3.04	6.94	0.00	5.06	5.41
Vesuvius?	11.34	6.48	8.30	9.90	5.74	4.94	8.45	0.00	8.22	6.91
	502 nm	537 nm	540 nm	545 nm	565 nm	590 nm	610 nm	640 nm	670 nm	714 nm
Canada	7.66	6.59	0.00	1.78	7.09	6.96	7.01	10.06	22.99	11.76
Persia	9.08	0.00	4.18	14.72	8.22	10.25	11.31	10.28	11.46	12.79
Afghanistan	10.93	2.02	0.00	22.78	2.91	15.11	25.00	2.18	127.53	36.86
Chile	7.71	1.52	10.02	0.00	9.41	10.85	9.15	10.84	9.46	7.52
Vesuvius?	9.58	0.00	16.94	0.00	8.81	11.07	12.09	10.55	24.50	8.92